Bit Error Ratio Performance of 112 Gb/s PM-QPSK Transmission Systems

John C. Cartledge, *Fellow, IEEE*, John D. Downie, Jason E. Hurley, Xiaming Zhu, and Ioannis Roudas

Abstract—**For 112 Gb/s polarization-multiplexed quadrature-phase-shift-keying systems, the generalized Gaussian probability density function is used to quantify the impact of carrier phase estimation algorithms on the statistical properties of the resultant signal sample values and to obtain an estimate of the system bit error ratio when direct bit error counting is not feasible. The shape parameter in the probability density function is useful for distinguishing the performance of different signal processing algorithms and system configurations.**

Index Terms—**Bit error ratio (BER), coherent optical transmission, signal processing.**

I. Introduction

FOR coherent optical transmission systems, the polarization-multiplexed quadrature-phase-shift-keying (PM-QPSK) modulation format is widely used for a bit rate of 100 Gb/s as it provides an appropriate compromise between spectral efficiency, required optical signal-to-noise ratio (OSNR), and modulated signal bandwidth for systems with forward error correction (FEC) coding and a 50 GHz channel spacing [1]. The combination of coherent detection, analog-to-digital conversion, and digital signal processing has proven to be particularly powerful. Coherent detection preserves both the amplitude and phase of the received optical signal in the photodetected signal and, thus, allows for signal processing that effectively mitigates linear transmission impairments and implements key receiver functions.

Numerical investigations of PM-QPSK system performance (simulations and experiments with off-line signal processing) frequently use direct bit error counting to determine the bit error ratio (BER). The corresponding Q-factor is calculated using the inverse complementary error function. This approach can only be used for system configurations that have a BER that is large enough to be determined with reasonable computational processing times. For system configurations where the BER is too small for direct bit error counting to be practical, the conditional moments of the signal sample values at the input to the decision function can be used to determine the specific form of an assumed probability density function. For example, means and variances can be used to specify Gaussian probability density functions. However, the accuracy of the Gaussian approximation depends on the specific system configuration. Furthermore, the extent and complexity of the signal processing in a coherent receiver make it difficult to derive a complete statistical description of the signals at the input to the decision function.

In this paper, the generalized Gaussian probability density function is investigated as a means of 1) quantifying the impact of carrier phase estimation algorithms on the statistical properties of the resultant signal sample values and 2) obtaining an estimate of the system performance with a limited increase in computational complexity when direct bit error counting is not feasible. It is shown that the shape parameter of the generalized Gaussian probability density function depends on the carrier phase estimation algorithm and, to a lesser extent, on the algorithm parameter values.

II. BER Performance

The generalized Gaussian probability density function is given by [4]

$$f(x;\mu,\sigma,p) = \frac{1}{2\Gamma(1+1/p)A(p,\sigma)} \exp\left\{-\left[\frac{|x-\mu|}{A(p,\sigma)}\right]^p\right\} \tag{1}$$

where

$$A(p,\sigma) = \left[\frac{\sigma^2\Gamma(1/p)}{\Gamma(3/p)}\right]^{1/2} \tag{2}$$

μ is the mean, σ^2 is the variance, p is the shape parameter, and Γ is the gamma function. The Gaussian probability density function is obtained for $p = 2$. When $p < 2$, as is frequently the case here, the tail probabilities are increased relative to the Gaussian density.

Several techniques for determining the value of the shape parameter p for a generalized Gaussian probability density function have been reported [2]–[6]. Most of these are based on values for the statistical moments of the random variable of interest. It has been shown that for systems without optical dispersion compensation, the four components of a PM-QPSK signal (in-phase X polarization, in-phase Y polarization, quadrature X polarization, quadrature Y polarization) are Gaussian distributed (or at least nearly Gaussian distributed) and statistically independent both before and after the digital signal processing in the receiver [7]. This applies to signals in the linear and nonlinear propagation regimes in the absence of amplified spontaneous emission (ASE) noise. Thus, a QPSK constellation can

Manuscript received September 14, 2011; revised November 09, 2011; accepted December 26, 2011. Date of publication February 07, 2012; date of current version April 04, 2012. This work was supported by the Natural Sciences and Engineering Research Council of Canada.

J. C. Cartledge was with Corning Inc., Corning, NY 14831 USA, on leave from the Department of Electrical and Computer Engineering, Queen's University, Kingston, ON K7L 3N6, Canada (email: john.cartledge@queensu.ca).

J. D. Downie, J. E. Hurley, X. Zhu, and I. Roudas are with Corning Inc., Corning, NY 14831 USA (email: downiejd@corning.com; hurleyje@corning.com; zhux@corning.com; roudasi@corning.com).

Color versions of one or more of the figures in this paper are available online at http://ieeexplore.ieee.org.

Digital Object Identifier 10.1109/JLT.2012.2186788

be decomposed into two binary-phase-shift-keying constellations (0 and π), or equivalently two ASK[1] constellations (-1 and $+1$), for the in-phase and quadrature components. When this decomposition is used to evaluate the BER, there are eight conditional density functions for a PM-QPSK signal (X and Y polarizations, in-phase and quadrature components, $+1$ and -1 transmitted bits), and hence, in principle, eight values of the shape parameter. To simplify the procedure, an alternative approach is used here that yields a single value of the shape parameter. When the BER is known from direct bit error counting, the value of p is obtained by equating the known BER to the calculated BER according to

$$\begin{aligned} BER &= 0.5\sum_n \left[\Pr(S_n > 0| -1) + \Pr(S_n \leq 0| +1)\right] \\ &= 0.5\sum_n \left[\int_0^\infty f_-(x;\mu_n,\sigma_n,p)dx + \right. \\ &\quad \left. \int_{-\infty}^0 f_+(x;\mu_n,\sigma_n,p)dx\right] \end{aligned} \tag{3}$$

where $n = IX, QX, IY, QY$ and the subscripts $I, Q, X, Y, +$ and $-$ denote the in-phase and quadrature components, X and Y polarizations, and $+1$ and -1 transmitted bits, respectively. $\Pr(S_n > 0\,|, -1)$ represents the conditional probability of error for the signal S_n given a -1 transmitted bit and $\Pr(S_n \leq 0\mid +1)$ represents the conditional probability of error for S_n given a $+1$ transmitted bit. f_- and f_+ denote the conditional probability density functions given the transmitted bit. The left-hand side of (3) is the BER obtained by direct error counting (simulation or experiment with offline processing) and the right-hand side is the calculated BER using (1) and (2). Equation (3) assumes rectilinear decision regions and can be modified accordingly for different decision boundaries. When the BER is too small to obtain by direct bit error counting, it can be estimated using the conditional moments of the signal sample values and evaluation of the right-hand side of (3) with an appropriate value of p. In this case, a value of p can be inferred from results for similar system configurations by varying a suitable system parameter (e.g., OSNR, fiber length, per-channel launch power) to obtain the BER by direct error counting and then applying (3). While the value of p depends on the specific details of a given system configuration, using an inferred value is expected to provide improved accuracy in estimating BER compared to simpler approaches such as the Gaussian approximation.

III. Experimental Setup

The experimental setup is shown in Fig. 1. Four distributed feedback lasers with nominal linewidths of 5 MHz and spaced by 50 GHz were multiplexed together and modulated by a QPSK modulator driven by two $2^{15}-1$ pseudorandom bit sequences at 28 GSym/s (allowing for the FEC coding overhead). The output signal from the modulator was polarization multiplexed. The PM-QPSK signals were launched into a recirculating loop which had three spans with each span comprised of 100 km of a developmental ultralow-loss, large effective area fiber, and 100 km of ultralow-loss single-mode fiber. The span loss was compensated by a single-stage erbium-doped fiber amplifier and backward-pumped distributed Raman amplifier. A loop synchronous polarization scrambler was used to mitigate possible loop polarization effects. The measured channel was amplified and filtered (0.4 nm bandwidth) before detection by a polarization- and phase-diverse coherent receiver that used a local oscillator laser with a nominal linewidth of 100 kHz. The four signals from the balanced photodetectors were digitized by 50 GSa/s analog-to-digital converters using a real-time sampling oscilloscope with 20 GHz electrical bandwidth. The offline signal processing included 1) quadrature imbalance compensation [8]; 2) upsampling to 56 GSa/s and chromatic dispersion compensation using a fixed time- or frequency-domain equalizer; 3) digital square and filter timing recovery [9]; 4) polarization recovery, polarization mode dispersion compensation, and residual dispersion compensation using 15-tap adaptive equalizers in a butterfly configuration and the constant modulus algorithm [10], [11]; 5) carrier frequency recovery using a spectral domain algorithm [12]; 6) carrier phase recovery using four algorithms; and 7) symbol decisions. The carrier phase recovery was performed using the predecision [13], decision-aided maximum-likelihood (DA-ML) [14], fourth power with zero lag smoothing (ZLS) [15] and second-order phase-locked loop [16] algorithms. These algorithms involve removing the modulation from the total phase of the signal and filtering (i.e., averaging) to reduce the impact of ASE noise on the estimation of the relatively slowly varying laser phase noise. The BER was obtained by direct bit error counting. With suitable values for the parameters in the signal processing algorithms, cycle slips were not observed. Consequently, differential coding was not used.

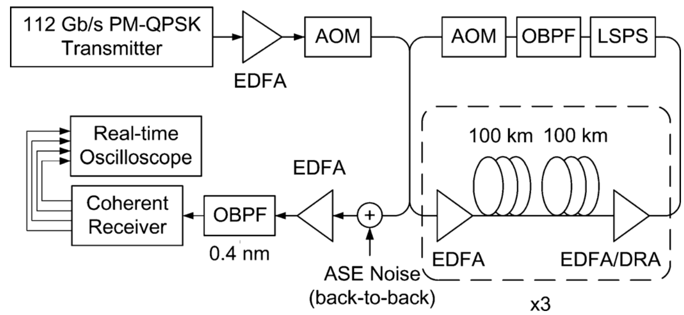

Fig. 1. Experimental setup. AOM: acousto-optic modulator. EDFA: erbium-doped fiber amplifier. DRA: distributed Raman amplifier. LSPS: loop synchronous polarization scrambler. OBPF: optical bandpass filter. ASE: amplified spontaneous emission.

IV. Results

For each system configuration, the offline signal processing was performed for five sets of data, with each dataset corresponding to 112 000 symbols. In comparing the phase noise estimation algorithms, the same five sets of data were used for each algorithm.

Fig. 2 illustrates the dependence of the average value of the shape parameter obtained for the five datasets on the transmitted power for the four carrier phase estimation algorithms. The corresponding BERs are also shown. The transmission distance is 2400 km. The BER performance is remarkably similar for the four algorithms despite the differences in the statistical properties of the signal sample values as indicated by the values of the shape parameter. The performance is limited by the OSNR for

[1]BPSK: binary-phase-shift-keying. ASK: amplitude-shift-keying.

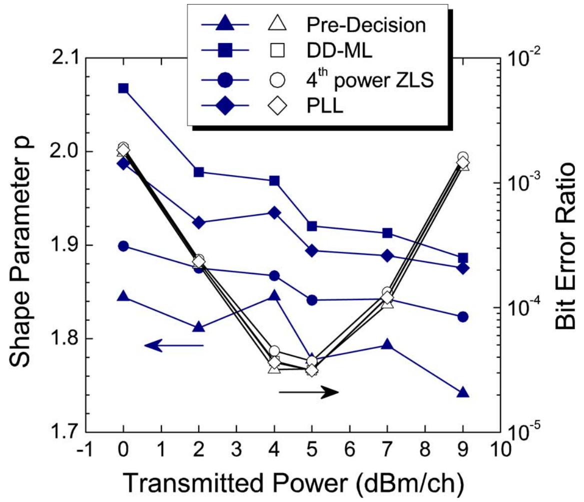

Fig. 2. Dependence of the average shape parameter (closed symbols) and BER (open symbols) on the transmitted power per channel for the four carrier phase estimation algorithms. The transmission distance is 2400 km.

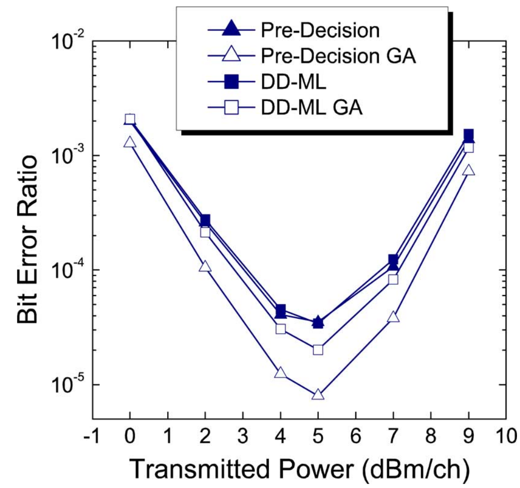

Fig. 4. Dependence of the BER on the transmitted power per channel for the predecision and DA-ML carrier phase estimation algorithms using bit error counting (closed symbols) and the Gaussian approximation (GA, open symbols). The transmission distance is 2400 km.

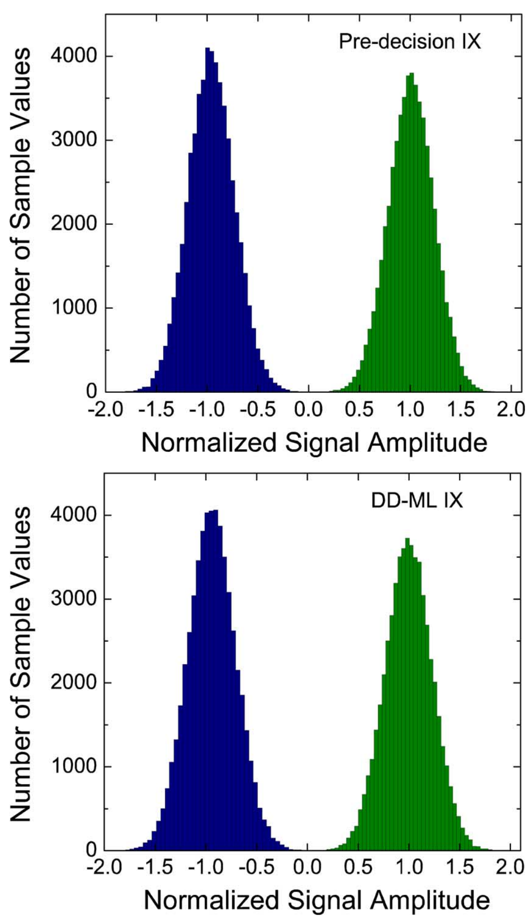

Fig. 3. Histograms for the sample values for the in-phase component of the X polarization signal. Transmitted power is 5 dBm/ch.

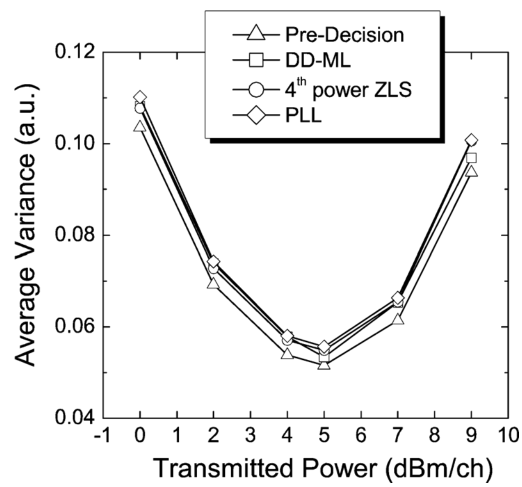

Fig. 5. Dependence of the average variance on the transmitted power per channel for the four carrier phase estimation algorithms. The transmission distance is 2400 km.

small transmitted powers and by fiber nonlinearities for large powers.

Histograms for the in-phase component of the X polarization signal are compared in Fig. 3 for the predecision and DA-ML phase estimation algorithms. Since this signal is equivalent to an ASK signal, the conditional mean and variance are determined from the sample values corresponding to -1 and $+1$. The conditional mean and variance are (1.012, 0.053) for the $+1$ bits and $(-0.960, 0.054)$ for the -1 bits for the predecision algorithm, and (0.996, 0.056) for the $+1$ bits and $(-0.944$, 0.058) for the -1 bits for the DA-ML algorithm. The differences in the histograms, and, hence, the means and variances, lead to the different values of the shape parameter. Fig. 4 illustrates the impact of the shape parameter on the BER by comparing the predecision and DA-ML results from Fig. 2 (bit error counting) with corresponding results obtained using the conditional means and variances for the sample values for the four signals (IX, QX, IY, and QY) and the Gaussian approximation $(p = 2)$. The Gaussian approximation underestimates (over estimates) the BER when $p < 2$ $(p > 2$, respectively). For a transmitted power of 5 dBm/ch, the underestimation is by factors of 4.1 and 1.6 for the predecision and DA-ML algorithms, respectively.

The usefulness of the generalized Gaussian probability density function is further demonstrated in Fig. 5 which shows the dependence of the average variance on the transmitted power for the four carrier phase estimation algorithms. For each value

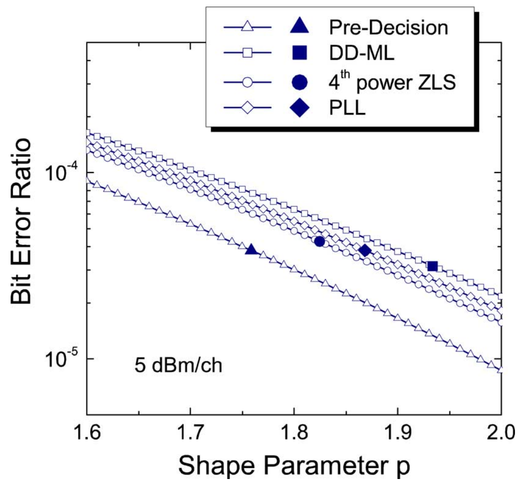

Fig. 6. Dependence of the BER on the shape parameter for a single dataset and the four carrier phase estimation algorithms. The solid symbols indicate the values obtained from (3).

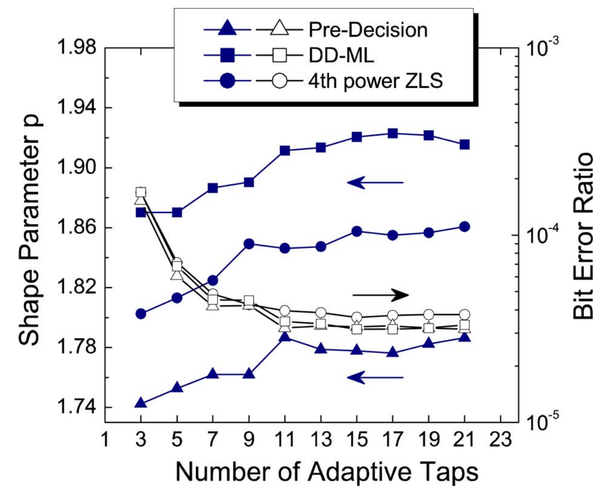

Fig. 8. Dependence of the shape parameter and BER on the number of taps for the adaptive equalizer (with a filter length of 16 for the predecision and DA-ML algorithms, and 33 for the fourth power ZLS algorithm). The transmission distance is 2400 km.

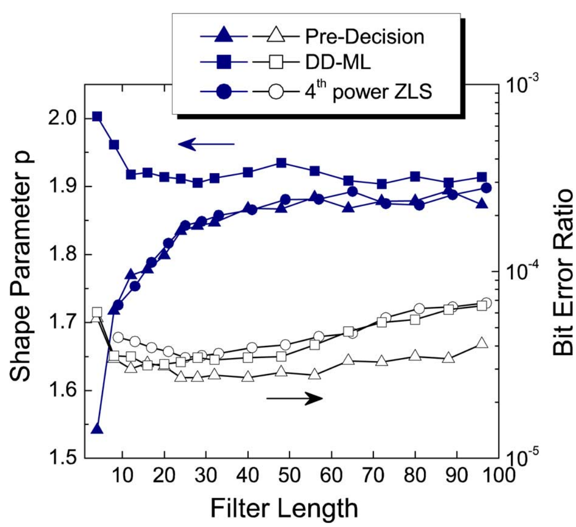

Fig. 7. Dependence of the shape parameter and BER on the filter length for the predecision, DA-ML, and fourth power ZLS algorithms (with 15 taps for the adaptive equalizer). The transmission distance is 2400 km.

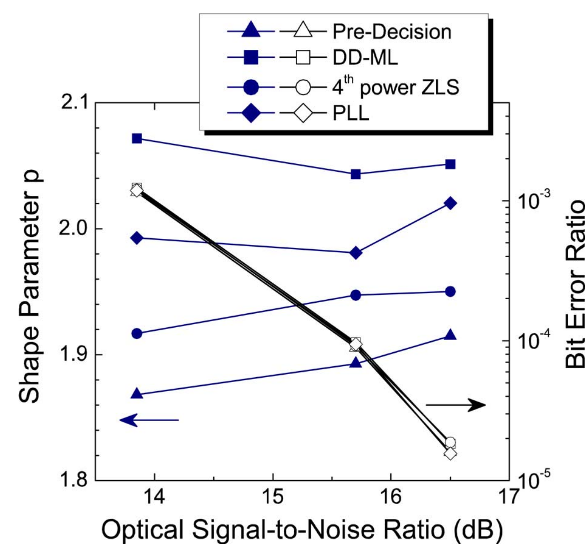

Fig. 9. Dependence of the average shape parameter and BER on the OSNR for a back-to-back system configuration and the four carrier phase estimation algorithms.

of the transmitted power, the average variance is obtained by averaging the variances for the eight conditional density functions (X and Y polarizations, in-phase and quadrature components, $+1$ and -1 transmitted bits) and the five sets of data. Interestingly, the shape parameter distinguishes the OSNR-limited results from the fiber-nonlinearity-limited results (see Fig. 2) whereas the average variance does not.

The sensitivity of the calculated BER to the value of the shape parameter over the range 1.6–2.0 is shown in Fig. 6 for a single dataset and the four carrier phase estimation algorithms. The transmission distance is 2400 km and the launch power is 5 dBm/ch. The solid symbols indicate the values obtained from (3). The change in BER over this range of p values is similar for the four algorithms varying by about a factor of 10. The extent to which the signal sample values are Gaussian distributed (results for $p = 2$) depends on the carrier phase estimation algorithm.

The value of the shape parameter obtained from (3) also depends to some extent on other aspects of the signal processing. This is shown in Figs. 7 and 8 for the predecision, DA-ML, and fourth power ZLS algorithms. The dependence of the shape parameter and BER on the averaging (i.e., filter length) in the carrier phase estimation algorithms (with 15 taps for the adaptive equalizer) and on the number of taps for the adaptive equalizer (with a filter length of 16 for the predecision and DA-ML algorithms, and 33 for the fourth power ZLS algorithm) is shown. The shape parameter is more strongly dependent on the averaging in the carrier phase estimation algorithm than the number of taps in the adaptive equalizer. Importantly, in the regions of practical interest (near optimum performance), the change in the value of the shape parameter is relatively small.

Results for a back-to-back system configuration were also obtained. Fig. 9 illustrates the dependence of the average value of the shape parameter and BER (closed symbols) on the OSNR (0.1 nm noise bandwidth) for the four carrier phase estimation algorithms. As in Fig. 2, the BER performance is remarkably

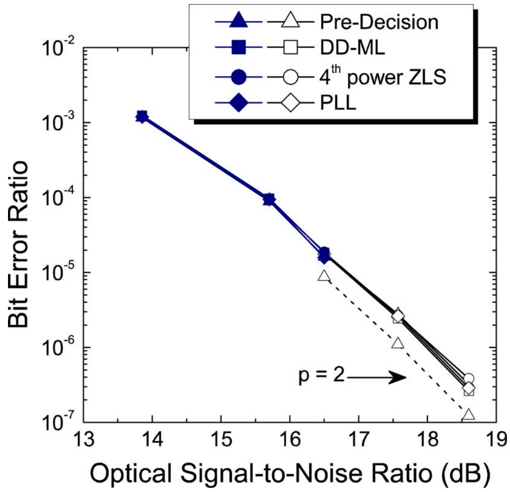

Fig. 10. Dependence of the BER on the OSNR for the four carrier phase estimation algorithms. The BER results are obtained by direct error counting (closed symbols and solid lines) and by the generalized Gaussian probability density function (open symbols and solid lines). For comparison, BER results are also shown for the predecision algorithm and Gaussian probability density function (open symbols and dashed line).

similar for the four algorithms despite the differences in the statistical properties of the signal sample values. Fig. 10 shows the BER results from Fig. 9 (obtained by direct bit error counting) and predicted values of the BER (open symbols) for OSNR values of 16.5, 17.6, and 18.6 dB. The predicted values were obtained from (3) and the conditional means and variances of the sample values for the four signals (IX, QX, IY, and QY). For these calculations, the values of p for an OSNR of 15.7 dB were used. For an OSNR of 16.5 dB, the total number of bit errors is in the range 35–42 depending on the carrier phase estimation algorithm, hence the corresponding values of the shape parameter are less reliable than those obtained for smaller values of the OSNR. Fig. 10 also illustrates predicted values of the BER for the predecision algorithm using the Gaussian approximation (open symbols and dashed line, $p = 2$). As expected, the Gaussian approximation underestimates the BER resulting in a discontinuity between the results obtained for direct bit error counting (low OSNR) and numerical prediction (high OSNR).

V. Conclusion

An approximation based on the generalized Gaussian probability density function has been investigated as a means of 1) quantifying the impact of carrier phase estimation algorithms on the statistical properties of the resultant signal sample values and 2) obtaining an estimate of the system performance when direct bit error counting is not feasible. While the four carrier phase estimation algorithms yield similar BER performance, the corresponding shape parameters for the generalized Gaussian probability density function are distinct. For 2400 km transmission, the shape parameter varies from 1.78 (predecision) to 1.92 (DA-ML) at the optimum launch power of 5 dBm/ch.

Although it is common practice to add ASE noise at the receiver in order to determine the OSNR sensitivity of a system for a BER corresponding to the FEC threshold, it is also of interest to estimate the actual system performance without the noise loading. When the BER is too small to obtain by direct bit error counting because of the required computational processing times, it can be estimated using the conditional moments of the signal sample values and an appropriate value of the shape parameter. This value can be obtained by varying a suitable system parameter (e.g., OSNR, fiber length, per-channel launch power) in the system configuration of interest. For example, for a large OSNR, the shape parameter can be estimated from BER results for smaller OSNRs. Similarly, although not shown here, for a short fiber length the shape parameter can be estimated from BER results for longer fiber lengths. Given the statistical variability in determining the shape parameter, specifying it in increments of 0.05 (e.g., 1.80, 1.85, 1.90, ...) provides a good compromise between this uncertainty and the resultant accuracy of the BER estimates.

References

[1] K. Roberts, M. O. Sullivan, K.-T. Wu, H. Sun, A. Awadalla, D. J. Krause, and C. Laperle, "Performance of dual-polarization QPSK for optical transport systems," *J. Lightw. Technol.*, vol. 27, no. 16, pp. 3546–3559, Aug. 2009.
[2] M. K. Varanasi and B. Aazhang, "Parametric generalized Gaussian density estimation," *J. Acoust. Soc. Amer.*, vol. 86, no. 4, pp. 1404–1415, 1989.
[3] S. B. Weinstein, "Estimation of small probabilities by linearization of the tail of a probability distribution function," *IEEE Trans. Commun.*, vol. COM-19, no. 6, pp. 1149–1155, Dec. 1971.
[4] M. C. Jeruchim, "Techniques for estimating the bit error rate in the simulation of digital communication systems," *IEEE Sel. Areas Commun.*, vol. SAC-2, no. 1, pp. 153–170, Jan. 1984.
[5] J, A. Domínguez-Molina and , J. A. , G. González-Farías, and R. Rodríguez-Dagnino, "A practical procedure to estimate the shape parameter in the generalized Gaussian distribution,". [Online] [Online]. Available: www.cimat.mx/reportes/enlinea/I-01-18_eng.pdf
[6] N. Stojanovic, "Tail extrapolation in MLSE receivers using nonparametric channel model estimation," *IEEE Trans. Signal Process.*, vol. 57, no. 1, pp. 270–278, Jan. 2009.
[7] A. Carena, G. Bosco, V. Curri, P. Poggiolini, M. T. Taiba, and F. Forghieri, "Statistical characterization of PM-QPSK signals after propagation in uncompensated fiber links," in *Proc. Eur. Conf. Opt. Commun.*, 2010, Paper P4.07.
[8] I. Fatadin, S. J. Savory, and D. Ives, "Compensation of quadrature imbalance in an optical QPSK coherent receiver," *IEEE Photon. Technol. Lett.*, vol. 20, no. 20, pp. 1733–1735, Oct. 2008.
[9] H. Meyer, M. Moeneclaey, and S. A. Fechtel, *Digital Communications Receivers*. New York: Wiley-Interscience, 1997, section 5.4.
[10] J. R. Treichler and B. G. Agee, "A new approach to multipath correction of constant modulus signals," *IEEE Trans. Acoust., Speech, Signal Process.*, vol. ASSP-31, no. 2, pp. 459–472, Apr. 1983.
[11] S. J. Savory, "Digital filters for coherent receivers," *Opt. Exp.*, vol. 16, no. 2, pp. 804–817, 2008.
[12] M. Morelli and U. Mengali, "Feedforward frequency estimation for PSK: A tutorial review," *Eur. Trans. Telecommun.*, vol. 9, no. 2, pp. 103–116, 1998.
[13] Z. Tao, L. Li, A. Isomura, T. Hoshida, and J. C. Rasmussen, "Multiplier-free phase recovery for optical coherent receivers," in *Proc. Opt. Fiber Commun. Conf.*, 2008, pp. 1–3.
[14] S. Zhang, P. Y. Kam, C. Yu, and J. Chen, "Decision-aided carrier phase estimation for coherent optical communications," *J. Lightw. Technol.*, vol. 28, no. 11, pp. 1597–1607, Jun. 2010.
[15] M. G. Taylor, "Phase estimation methods for optical coherent detection using digital signal processing," *J. Lightw. Technol.*, vol. 27, no. 7, pp. 901–914, Apr. 2009.
[16] I. Fatadin, D. Ives, and S. J. Savory, "Compensation of frequency offset for differentially encoded 16- and 64-QAM in the presence of laser phase noise," *IEEE Photon. Technol. Lett.*, vol. 22, no. 3, pp. 176–178, Feb. 2010.

Author biographies not included at authors' request due to space constraints.